

# H inf. Loop Shaping Robust Control vs. Classical PI(D) Control: A case study on the Longitudinal Dynamics of Hezarfen UAV

KAMURAN TURKOGLU <sup>1</sup>

ELBROUS M. JAFAROV <sup>2</sup>

Department of Aeronautics and Astronautics,  
Istanbul Technical University, Istanbul, Turkey

Istanbul Teknik Universitesi, Ucak-Uzay Bilimleri Fakultesi, Maslak, 34469 Sariyer, Istanbul  
TURKEY

*Abstract:* - In this paper, the longitudinal dynamics and automatic control system design processes of Hezarfen UAV for longitudinal flight have been discussed. Hezarfen UAV is a prototype UAV aircraft which is being designed and going to be build-up for the first time in co-operation with Istanbul Technical University, Faculty of Aeronautics and Astronautics. In the first part of the paper, longitudinal dynamic properties of Hezarfen UAV have been presented. Following to that, automatic control system for the longitudinal flight (autopilot) has been designed using classical PID control algorithm, in the second part of the paper. In the third part, as an alternative, one-degree of freedom H inf. Loop Shaping Robust Control system has been suggested and implemented to the system. Obtained results are given in comparison and presented in the conclusions part of the paper.

*Key-Words:* - H inf. Loop Shaping, Robust Control, Classical Control, PID, UAV, Longitudinal Dynamics

## 1 Introduction

In the recent years, UAV's have widely been used in several areas such as reconnaissance, intelligence, border security, combat missions ... etc. In all of the specified missions, UAV's are demanded to work with high accuracy and precision. In that sense, the dynamic modeling and especially the automatic control system design are playing crucial roles in UAV's. As an approach to these, in literature there are quite a lot of control system design applications on UAV's like receding horizon control [1], variable horizon model predictive control [2], control system design using evolutionary algorithms [3], feedback linearization and linear observer design [4], cooperative receding horizon control [5], adaptive control system design [6], control system design using MIMO QFT [7], decentralized non-linear control [8], robust control system design using coupled stabilities [9], H infinity control and inverse dynamic system approach [10] and non-linear autopilot design using dynamic inversion [11] are some of the studies.

In the light of the given references, in this paper first of all, the longitudinal dynamics of UAV has been studied and afterwards automatic control system designs using H inf. Loop Shaping and classical PID control have been implemented separately on the nominal plant and observed results are discussed in detail in the conclusions section.

## 2 Longitudinal Flight Model of UAV

In longitudinal dynamics of the Hezarfen UAV, linearized and Laplace transformed Equations of Motion (EOM), taken from [12], has been used so that the EOMs for the longitudinal flight are presented as

$$\begin{aligned}
 \mathbf{x}: & \left( \frac{mu}{Sq} s - C_{X_u} \right) 'u(s) - C_{X_\alpha} ' \alpha(s) - C_w (\cos \Theta) \theta(s) = 0 \\
 \mathbf{z}: & -C_{Z_u} 'u(s) + \left[ \left( \frac{mu}{Sq} - \frac{c \cdot C_{Z\dot{\alpha}}}{2u} \right) s - C_{Z_\alpha} \right] ' \alpha(s) \\
 & + \left[ \left( -\frac{mu}{Sq} - \frac{c \cdot C_{Zq}}{2u} \right) s - C_w \sin \Theta \right] \theta(s) = 0 \\
 \mathbf{M}: & \left( -\frac{c \cdot C_{m\dot{\alpha}}}{2u} s - C_{M_\alpha} \right) ' \alpha(s) + \left( \frac{I_y}{Sq c} s^2 - \frac{c \cdot C_{M_q}}{2u} s \right) \theta(s) = 0
 \end{aligned} \tag{1}$$

where

'u = Change of velocity in longitudinal flight  
'α = Change of angle of attack in longitudinal flight  
θ = Change of pitching angle from the equilibrium condition

and

$$'u = \frac{u}{U_0}, \quad ' \alpha = \frac{w}{U_0}$$

where

u = Velocity in X direction  
w = Velocity in Z direction

The characteristic properties of Hezarfen UAV and stability derivatives are presented and calculated in Table 1 and Table 2, respectively [13].

$m = 5$ [kg]
$U_0 = 12$ [m/sec]
$g = 9.807$ [m/sec <sup>2</sup> ]
$S_{wing} = 0.4205$ [m <sup>2</sup> ]
$S_{vertical\ tail} = 0.1323$ [m <sup>2</sup> ]
$\rho = 1.226$ [kg/m <sup>3</sup> ]
$I_{yy} = 0.1204$ [m <sup>4</sup> ]
$c = 0.235$ [m]

**Table 1** Characteristic properties of UAV.

$C_{x_u} = -0.0264$	$C_{Z_{\dot{\alpha}}} = -0.0347$
$C_{x_{\alpha}} = 1.2821$	$C_{Z_{\alpha}} = -0.1381$
$C_D = 0.0132$	$C_{Z_q} = -3.30$
$C_L = 1.3210$	$C_{M_{\dot{\alpha}}} = -0.0347$
$C_W = -1.3210$	$C_{M_{\alpha}} = -0.0312$
$L_{l/c} = 1$	$C_{M_q} = -3.30$
$C_{Z_u} = -2.6421$	$C_{X_{\delta_e}} = 0$
$C_{Z_{\delta_e}} = -0.71$	$C_{m_{\delta_e}} = -0.71$

**Table 2** Stability derivatives and inputs of UAV.

Using the characteristic properties given in Table 1 and calculated stability derivatives given in Table 2 and profiting from (1), it is possible to obtain the matrix representation of longitudinal flight as

$$\begin{bmatrix} (1.6165 + 0.0264s) & -1.2821 & 1.3210 \\ 2.6421 & (1.6168s + 0.1381) & -1.4460s \\ 0 & (0.0003s + 0.0312) & (0.0138s^2 + 0.0323s) \end{bmatrix} \begin{bmatrix} 'u(s) \\ '\alpha(s) \\ \theta(s) \end{bmatrix} = \begin{bmatrix} 0 \\ -0.71 \\ -0.71 \end{bmatrix} \quad (2)$$

Using (2), it is relatively easy to obtain the corresponding transfer functions (TFs) ( $'u/\delta_e$ ,  $'\alpha/\delta_e$ ,  $\theta/\delta_e$ ). Due to the reason that the properties of longitudinal flight is taken into consideration in the paper, only  $\theta/\delta_e$  TF will be discussed in the following parts. The corresponding TF is gained as

$$\frac{\theta(s)}{\delta_e(s)} = \frac{1.855s^2 + 0.153s + 2.407}{0.036s^4 + 0.0889s^3 + 0.1354s^2 + 0.1121s + 0.109} \quad (3)$$

From (2), it is possible to obtain the location of the poles with the purpose of having a better idea about the open loop time domain response of the nominal UAV system [14]. If the poles of the system are investigated, they should be found as

$$\begin{aligned} s_{1,2} &= -1.2171 \pm 0.9737i \\ s_{3,4} &= -0.0164 \pm 1.1151i \end{aligned} \quad (4)$$

where  $s_1$  and  $s_2$  are representing the short period mode, and  $s_3$  and  $s_4$  are representing the phugoid (long period) mode in the longitudinal flight. If the corresponding natural frequency values and damping ratios are calculated, they could be determined as

phugoid mode	short period mode
$\xi_{pm} = 0.0147$	$\xi_{sp} = 0.7809$
$\omega_{n\_pm} = 1.1152$ rad/s	$\omega_{n\_sp} = 1.5587$ rad/s
$T_{pm} = 61.0687$ s	$T_{sp} = 0.8216$ s

Also, it is likely to see from the very close poles ( $s_{3,4}$ ) to the origin and from (5) that the damping in phugoid mode is relatively very low ( $\xi_{pm} \ll 1$  under-damped), which is leading to long lasting ( $T_{pm} = 61.06$  sec) and frequent oscillations ( $\xi_{pm} = 0.0147$ ) in the system. Moreover, with the intention of having a better idea of the longitudinal flight, Bode plot has been attained for frequency domain analysis and is given in Fig.1.

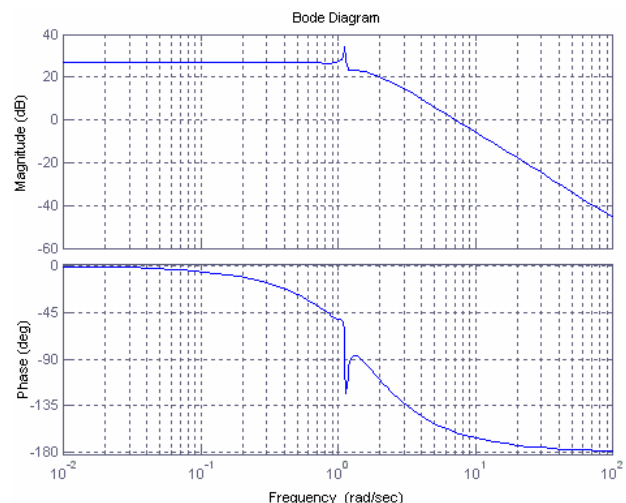


**Fig.1** Bode plot of  $\theta/\delta_e$ .

It is predictable from Fig.1 that the longitudinal flight is noticeably affected in phugoid mode ( $\omega_{n\_pm} = 1.1152$  rad/sec) due to a given elevator

deflection, as it is also expected from (4) and (5), as well. Furthermore, if the open loop time domain responses of change of pitch angle ( $\theta$ ) with respect to a given elevator deflection ( $\delta_e$ ) is plotted, it is probable to detect the responses as given in Fig.2, where Fig.2 represents the open loop (OL) time domain *step* response and the OL time domain *impulse* response of  $\theta/\delta_e$ , respectively.

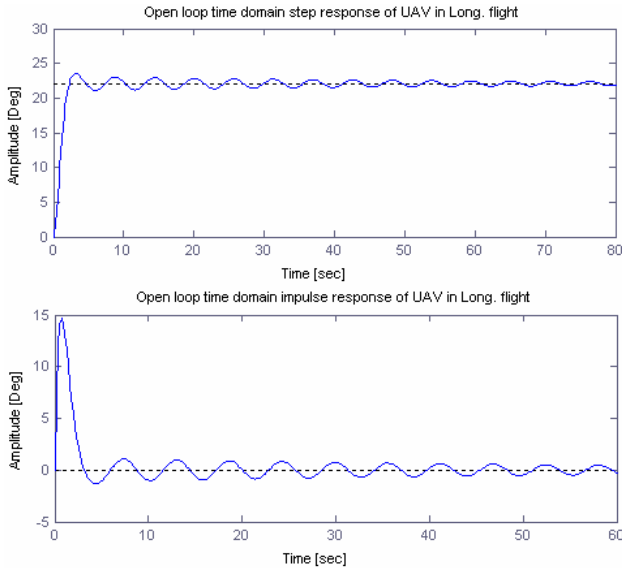


Fig.2 OL time domain responses of  $\theta/\delta_e$ .

From Fig.2, it is straightforward to see the low damping and the long lasting oscillations in the longitudinal flight of Hezarfen UAV system.

Due to all specified reasons, a nicely augmented control system design is significantly required in Hezarfen UAV longitudinal flight system. For that reason, in the following sections two different kind of (firstly PI(D) and secondly  $H_{\infty}$  Loop Shaping) control system design's have been given with comparison to each other.

### 3 PI(D) Control System Design

In this segment of the paper, PID control system design for the longitudinal flight of Hezarfen UAV has been discussed in detail.

The most important motivation in using the PID control system design for the Hezarfen UAV plant is that it is easy to apply and here the aim is to suppress the oscillatory effects and to minimize the considerably big settling time values. In that sense, the core seek is to shape the very close poles ( $s_{3,4}$ ) to the origin.

First of all, the Simulink block diagram for PID control system has been constructed as given in Fig.3.

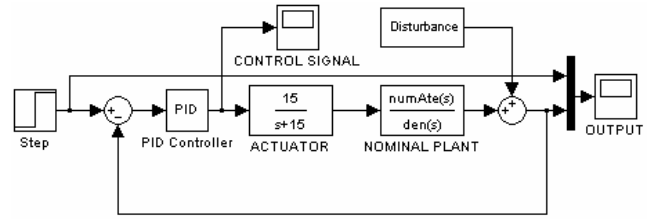


Fig.3 PID flight control system block diagram.

Using specified Ziegler-Nichols tuning charts in [15], after an iterative process, critical gain ( $K_{cr}$ ) and corresponding critical period ( $P_{cr}$ ) values have been obtained as  $K_{cr} = 0.1737$  and  $P_{cr} = 1.8$  sec. Using the obtained critical gain and corresponding critical period values the Proportional (P), Integral (I) and the Derivative (D) parts are obtained after an iterative process as  $P = 0.087$ ,  $I = 0.065$  and  $D = 0$  where widely used PID controller is defined as  $P = K_p$ ,  $I = K_p \frac{1}{T_i}$  and  $D = K_p T_d$  [15]. The derivative (D) part of PID control system has been neglected ( $D = 0$ ), because of under-damped poles ( $s_{3,4}$ ) of the system. When derivative part (D) is introduced into the system dynamics, the actuator signal is reaching to values such as  $10^{22}$  [N], which is an impossible force value for a dynamic system. This is occurring due to lightly damped poles ( $s_{3,4}$ ) of the system and when a derivative action is imposed to the system, the lightly damped poles are saturating the system. In the light of these, the PI control system's time domain response is found as given in Fig.4.

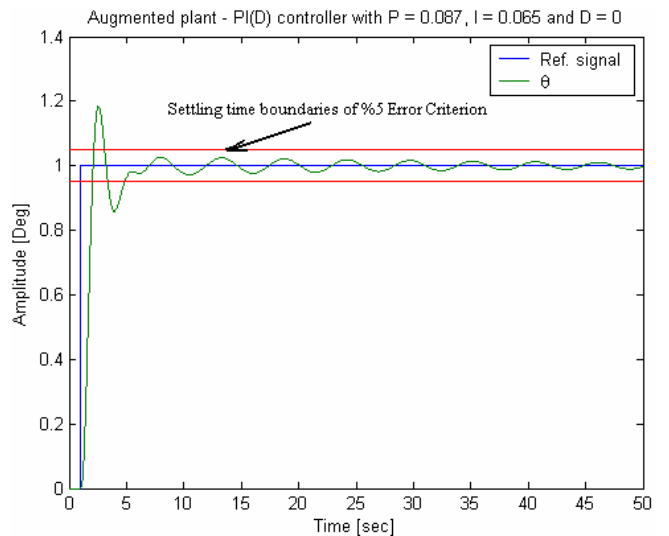


Fig.4 Time domain response of PID control system.

From Fig.4, it is likely to see that the settling time is  $\sim 5$ sec (regarding the 5% error criterion) and the maximum over-shoot  $\sim 18\%$ , which is within the

acceptable limits. If we check the control signal, the force imposed on the nominal plant by the actuator is shown in Fig.5.

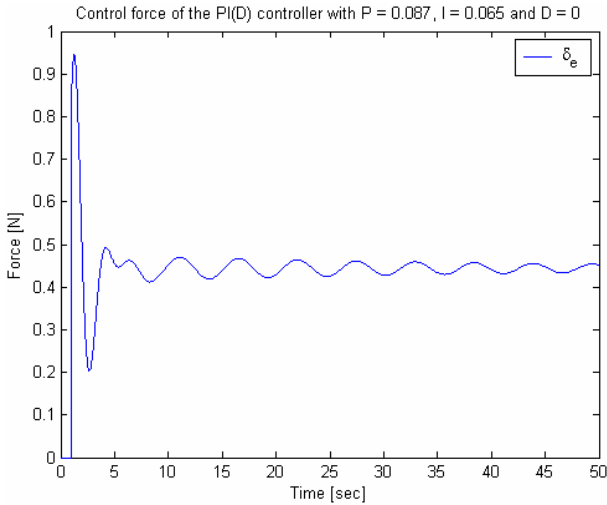


Fig.5 Control signal imposed by the actuator.

From Fig.5, it is able to observe that the maximum force acting on the elevators is  $\sim 0.95$  [N] ( $\sim 96$ grams), which is a considerable value regarding the weight (5kg) of the UAV. If the tracking and disturbance rejection of the PID controller is tested, the results are obtained as shown in Fig.6.

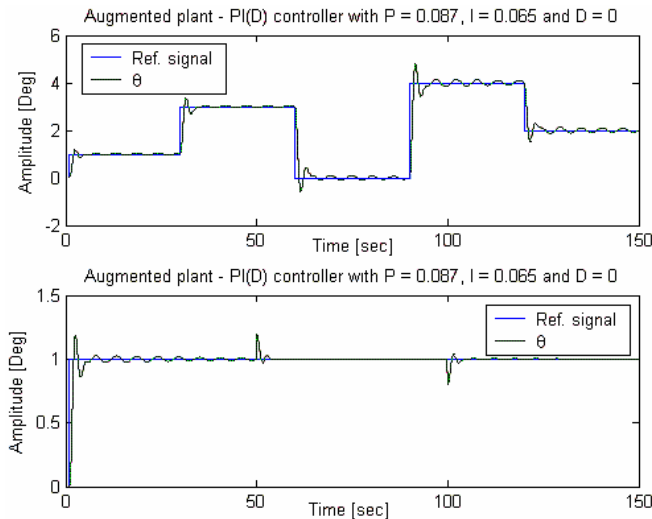


Fig.6 Tracking and disturbance rejection of PI(D) controller, respectively.

From Fig.6, the tracking of the PI(D) controller could be observed as acceptable and the disturbance rejection to a given 20% of disturbance regarding the reference signal is relatively good.

### 4 $H_\infty$ Loop Shaping Robust Control System Design

In this section, as an alternative to classical PID

control algorithm,  $H_\infty$  Loop Shaping Robust Control system application will be presented and obtained results will be compared to PI(D) control system's results, at the end of the paper.

$H_\infty$  Loop shaping is mainly based on weighting the corresponding inputs and outputs of the nominal plant, where it has several advantages regarding the classical methods [16]. First of all, in  $H_\infty$  Loop Shaping there is no  $\gamma$  iteration process. Secondly, it combines the performance benefits of the classical loop-shaping with robust characteristics of  $H_\infty$  optimization. Moreover, it is a straightforward method which has several application areas such as helicopters, VSTOL aircrafts, automotive industry, etc. It is also applicable to lightly damped modes (like it is in Hezarfen UAV system). For Hezarfen UAV system,  $H_\infty$  Loop Shaping Simulink block diagram has been constructed using recommended methods in [16] and is shown in Fig.7.

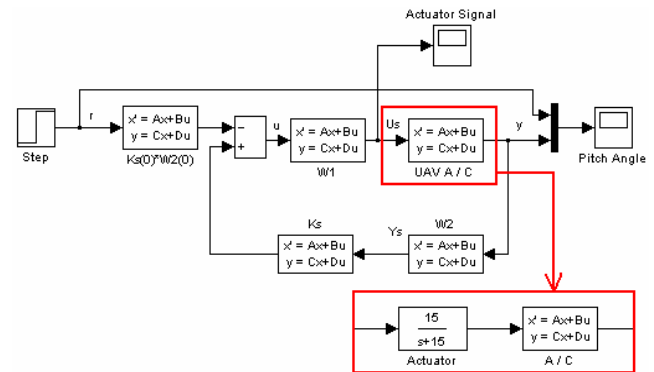


Fig.7  $H_\infty$  Loop Shaping control system block diagram.

After the construction of the block diagram of the feedback control system, the next step is to determine the weighting functions  $W_1$  and  $W_2$ . As a result of an iterative process, the least but not last, weighting transfer functions,  $W_1$  and  $W_2$ , have been obtained as

$$W_1 = \frac{4(8.9s + 8.9)}{8s + 0.1}, \quad W_2 = \frac{46}{s + 46} \quad (6)$$

By using the chosen transfer functions and with the help of Matlab `ncfsyn` command the maximum stability margin,  $e_{max}$ , could be found. Maximum stability margin is estimated as a performance criterion and is defined as  $e_{max} = 1/\gamma_{min}$ , where  $\gamma_{min}$  has been described as  $H_\infty$  optimal cost. Here the option of having an optimal controller has been selected by choosing `ncfsyn` factor equal to 1 [17]. Using all of the given information  $e_{max}$  is obtained as  $e_{max} = 0.2609$ , where the optimal value is

suggested as  $0.25 < e_{\max} < 0.3$ . After having a considerable stability margin it is time to check out the time domain responses of the augmented system. Using the preferred weighting functions  $W_1$  and  $W_2$ , the closed loop time domain response of  $H_\infty$  Loop Shaping robust control system is presented in Fig.8.

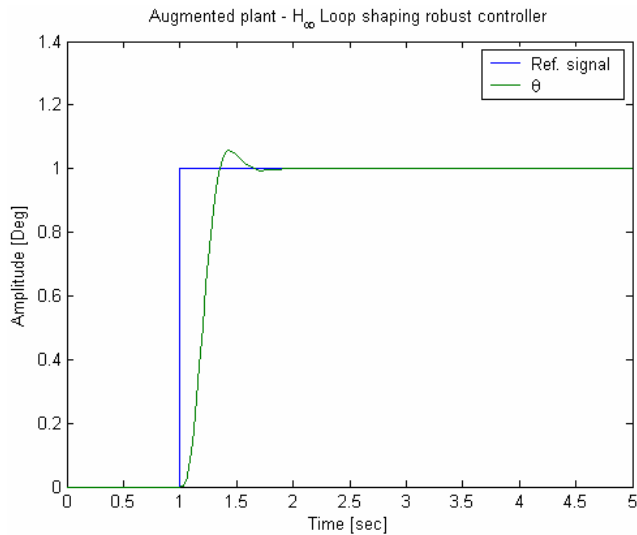


**Fig.8** Closed loop time domain response of  $H_\infty$  Loop Shaping robust control system.

As it is promising to see from Fig.8, the time domain response of  $H_\infty$  Loop Shaping robust control system is nearly perfect. The settling time is  $\sim 0.6$ sec and the maximum-overshoot is  $\sim 6\%$ , which are remarkably good and high-quality responses. Moreover, if the actuator force is plotted, it is obtained as presented in Fig.9.

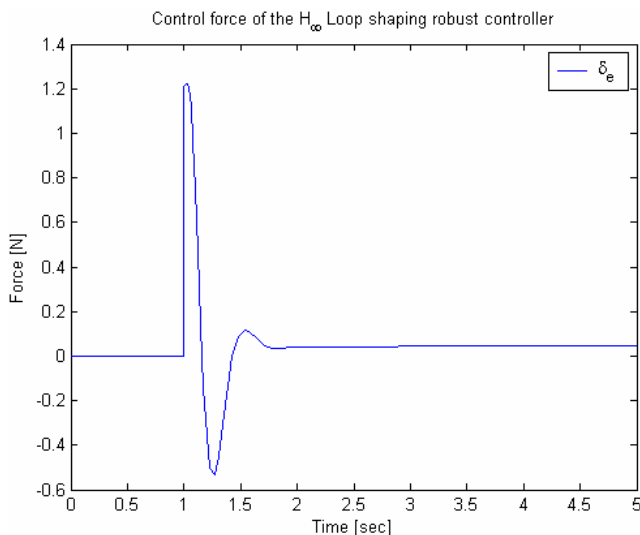


**Fig.9** Control force imposed by the actuator on the nominal plant.

From Fig.9, it could be observed that the maximum control force acting on the elevators is  $\sim 1.2$  [N]

( $\sim 122$ grams), which also a significant value regarding the weight (5kg) of the UAV. Furthermore, if the tracking and the disturbance rejection of the  $H_\infty$  Loop Shaping controller are investigated, the corresponding plots are attained as given away in Fig.10.

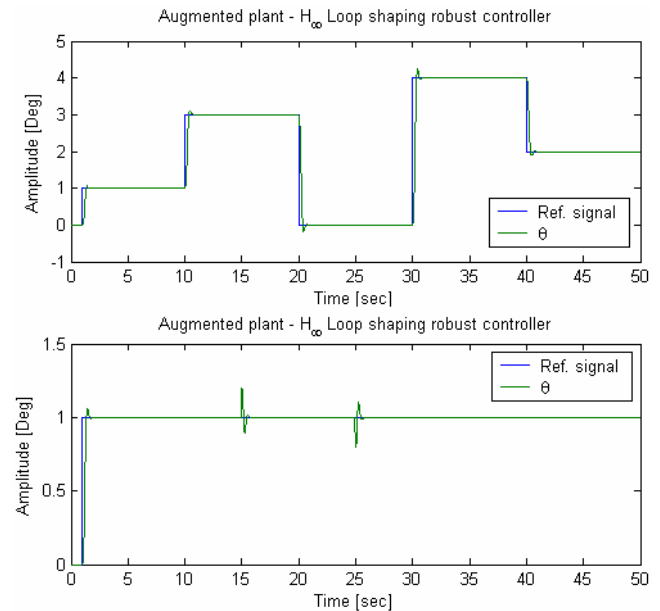


**Fig.10** Tracking and disturbance rejection of  $H_\infty$  Loop Shaping controller, respectively.

As it is likely to see from Fig.10, the tracking of loop shaping controller against different kind of step inputs is truly ideal and the disturbance rejection to given 20% of disturbance regarding the reference signal is actually superb. In order to have a better idea of time domain responses of both PID and  $H_\infty$  Loop Shaping control systems, they have been given in comparison to each other, in Fig.11.

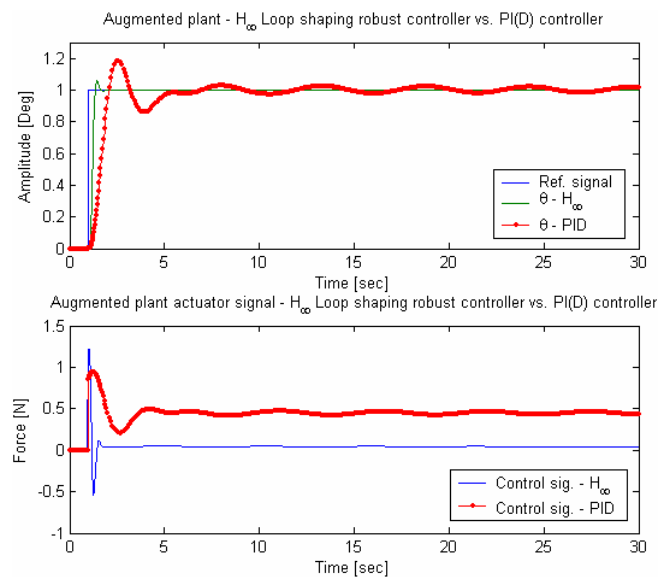


**Fig.11** Comparison of  $H_\infty$  Loop Shaping vs. PI(D).

From Fig.11, it easy to see the influence of loop shaping and weight augmentation via  $H_\infty$  Loop Shaping control system on Hezarfen UAV system. The performance, robustness and disturbance rejection of  $H_\infty$  loop shaping controller is significantly more authoritative than classical PI(D) control system design. From all of the listed results, it is possible to see that there are several advantages of using loop shaping and  $H_\infty$  optimization in SISO systems. The power of  $H_\infty$  Loop Shaping is also well known in MIMO systems and has been proved on several applications such as helicopters, VSTOL aircrafts, etc.

### 5 Conclusion

In this paper, as a first step, the longitudinal dynamics of Hezarfen UAV has been discussed and afterwards two different control system designs have been implemented on longitudinal flight of UAV: PI(D) and  $H_\infty$  Loop Shaping Robust control systems. PI(D) control has been introduced in the third section of the paper and following to that in the fourth section of the paper  $H_\infty$  Loop Shaping control algorithm has been implemented to the UAV system. It has been seen that the  $H_\infty$  Loop Shaping is a very powerful technique in SISO systems so that nearly all the performance criteria's resulted far away better than the results of the PI(D) control system's one's, as it has been shown in Table 3.

Method	Settling Time	Max. Overshoot	Control Signal
PI(D)	5sec	18 %	1 [N]
$H_\infty$	0.6 sec	6 %	1.2 [N]

**Table 3** Performance values of PI and  $H_\infty$  controller

Also, regarding the disturbance rejection and robustness performances, it could also be understood that the authority of  $H_\infty$  Loop Shaping on the system was more convincing and trustworthy than the specified outcomes of PI(D) control system.

#### References:

[1] Keviczky, T. and Balas, G.J., Software-enabled receding horizon control for autonomous unmanned aerial vehicle guidance, *Journal of Guidance Control and Dynamics*, Vol. 29, No. 3, 2006, pp.680-694.  
 [2] Richards, A. and How, J.P., Robust variable horizon model predictive control for vehicle maneuvering, *International Journal of Robust and Non-Linear Control*, Vol.16, No.7, 2006, pp.333-351.  
 [3] Khantsis, S. and Bourmistrova, A., UAV controller design using evolutionary algorithms, *Advances in*

*Artificial Intelligence Lecture Notes in Artificial Intelligence*, No.3809, 2005, pp.1025-1030.  
 [4] Mokhtari A., M'Sirdi N.K., Meghrich K. and Belaidi A., Feedback linearization and linear observer for a quadrotor unmanned aerial vehicle, *Advanced Robotics*, Vol.20, No.1, 2006, pp.71-91.  
 [5] Li, W. and Cassandras, C.G., A cooperative receding horizon controller for multivehicle uncertain environments, *IEEE Transactions on Automatic Control*, Vol.51, No.2, 2006, pp.242-257.  
 [6] Fradkov, A. and Andrievsky, B., Combined adaptive controller for UAV guidance, *European Journal of Control*, Vol.11, No.1, 2005, pp.71-79.  
 [7] Kim, M.S. and Chung, C.S., The robust flight control of an UAV using MIMO QFT: GA-based automatic loop-shaping method, *Systems Modeling and Simulation: Theory and Applications Lecture Notes in Computer Science*, No.3398, 2005, pp.467-477.  
 [8] Singh, S.N., Zhang, R., Chandler, P. and Banda, S., Decentralized nonlinear robust control of UAVs in close formation, *International Journal of Robust and Non-Linear Control*, Vol.13, No.11, 2003, pp.1057-1078.  
 [9] Lombaerts, T.J.J., Mulder, J.A., Voorsluijs, G.M. and Decuypere, R., Design of a robust flight control system for a mini-UAV, *AIAA Guidance, Navigation, and Control Conference*, Vol.7, 2005, pp.5608-5626.  
 [10] Chen, Xin and Pan, Changchun, Application of H infinity control and inverse dynamic system in direct side force control of UAV, *Journal of Nanjing University of Aeronautics and Astronautics*, Vol.38, No.1, 2006, pp.33-36.  
 [11] Sadraey, M. and Colgren, R., Two DOF robust nonlinear autopilot design for a small UAV using a combination of dynamic inversion and H varies directly as loop shaping, *AIAA Guidance, Navigation, and Control Conference*, 2005, pp.5518-5538.  
 [12] Blakelock, J. H., *Automatic Control of Aircraft and Missiles*, Wiley, 1991.  
 [13] Turkoglu, K., Investigation the modes of Hezarfen UAV and automatic control systems design, *B.Sc. Graduation Thesis in Istanbul, Tech. Univ., Faculty of Aeronautics and Astronautics*, Supervised by Prof. E. M. Jafarov, 2006, pp.13-16.  
 [14] Turkoglu, K., Abdulhamitbilal, E., Tekin, R., Kale, S. and Jafarov, E. M., Longitudinal Dynamical modeling of Hazerfen UAV and PID Controller Design, *6<sup>th</sup> National Symposium on Aeronautics, Kayseri, Turkey*, 2006.  
 [15] Ogata, K., *Modern Control Engineering*, Prentice Hall, Third Edition, 1997, pp.670-673.  
 [16] Skogestad S. and Postlethwaite I, *Multivariable Feedback control*, Wiley, 1996.  
 [17] Turkoglu, K. and Jafarov, E. M., Lateral Robust Control System Designof Hezarfen UAV via  $H_\infty$  Loop Shaping Approach and Sensitivity / Co-Sensitivity Analysis, *WSEAS Transactions on Systems*, Issue 9, Vol.5, 2006, pp.2040-2048.